

# Soft Matter

Accepted Manuscript



This is an *Accepted Manuscript*, which has been through the Royal Society of Chemistry peer review process and has been accepted for publication.

*Accepted Manuscripts* are published online shortly after acceptance, before technical editing, formatting and proof reading. Using this free service, authors can make their results available to the community, in citable form, before we publish the edited article. We will replace this *Accepted Manuscript* with the edited and formatted *Advance Article* as soon as it is available.

You can find more information about *Accepted Manuscripts* in the [Information for Authors](#).

Please note that technical editing may introduce minor changes to the text and/or graphics, which may alter content. The journal's standard [Terms & Conditions](#) and the [Ethical guidelines](#) still apply. In no event shall the Royal Society of Chemistry be held responsible for any errors or omissions in this *Accepted Manuscript* or any consequences arising from the use of any information it contains.



## Soft Matter

## REVIEW

## Scaling up self-assembly: Bottom-up approaches to macroscopic particle organization

Received 00th January 20xx,  
Accepted 00th January 20xx

DOI: 10.1039/x0xx00000x

www.rsc.org/

M. H. Lash,<sup>a,d</sup> M. V. Fedorchak,<sup>a,b,c,d</sup> J. J. McCarthy,<sup>a,†</sup> and S. R. Little,<sup>a,b,d,e,†</sup>

This review presents an overview of recent work in the field of non-Brownian particle self-assembly. Compared to nanoparticles that naturally self-assemble due to Brownian motion, larger, non-Brownian particles ( $d > 6\mu\text{m}$ ) are less prone to autonomously organize into crystalline arrays. The tendency for particle systems to experience immobilization and kinetic arrest grows with particle radius. In order to overcome this kinetic limitation, some type of external driver must be applied to act as an artificial “thermalizing force” upon non-Brownian particles, inducing particle motion and subsequent crystallization. Many groups have explored the use of various agitation methods to overcome the natural barriers preventing self-assembly to which non-Brownian particles are susceptible. The ability to create materials from a bottom-up approach with these characteristics would allow for precise control over their pore structure (size and distribution) and surface properties (topography, functionalization and area), resulting in improved regulation of key characteristics such as mechanical strength, diffusive properties, and possibly even photonic properties. This review will highlight these approaches, as well as discuss the potential impact of bottom-up macroscale particle assembly. The applications of such technology range from customizable and autonomously self-assembled niche microenvironments for drug delivery and tissue engineering to new acoustic dampening, battery, and filtration materials, among others. Additionally, crystals made from non-Brownian particles resemble naturally derived materials such as opals, zeolites, and biological tissue (i.e. bone, cartilage and lung), due to their high surface area, pore distribution, and tunable (multilevel) hierarchy.

### 1.0. Introduction

Naturally occurring materials are elegant and sophisticated in structure, often with hierarchical features ranging in size from the nano- to macro- scales. The structural form, or architecture, of a material often dictates its function. For example, the highly regular brick-and-mortar layering of organic and inorganic elements in nacre (mollusk shell) create a strength, toughness, and hardness that makes nacre an excellent protective material for sea creatures due to the way stress propagates through it and energy is dissipated.<sup>1–3</sup> Similarly, the structural hierarchy of cells naturally present in cedar wood and lotus leaves highly favors efficient light harvesting due to the cellular organization, providing the ability to both focus and scatter light in different areas to maximize photosynthesis.<sup>4</sup> This tendency for the form or structure of a material to dictate its function is ubiquitously observed throughout the natural world, inspiring and challenging mimetic scientific design. Along these lines, hierarchy, ranging from the nano- to macro- scales, has been found to enhance material performance (e.g. strength, toughness, luminescence, electron and ion transfer,

etc.). In the design of synthetic materials, mimicking natural hierarchies may enhance the intrinsic properties and usability of the designed material.<sup>4–9</sup> Figure 1 shows naturally occurring materials with macroscale features. One such example is the macroscopic pore structure seen in native bone tissue that allows for the tissue to have high mechanical strength and low material density.<sup>6,8</sup> Similarly, the organization of photoreceptors in the drosophila (fruit fly) eye allows the insect to have a wide field of vision.<sup>10,11</sup> The organization and complexity of these structural features has inspired scientific study and mimetic design across many fields of research.

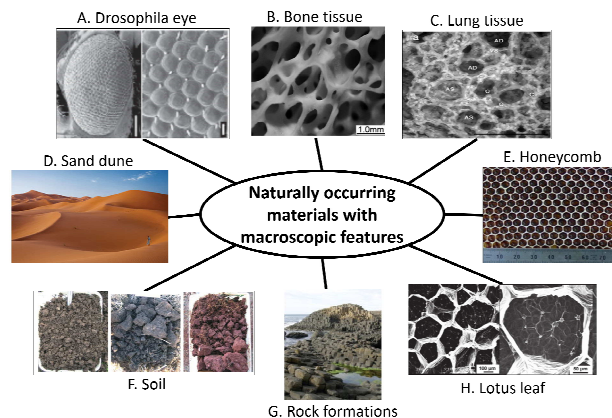


Figure 1: Naturally occurring materials with macroscopic features which directly impact the structures function and structural integrity. Part (A) and scale bars are 100 $\mu\text{m}$  and

<sup>a</sup> Department of Chemical and Petroleum Engineering.

<sup>b</sup> Department of Bioengineering.

<sup>c</sup> Department of Ophthalmology

<sup>d</sup> Department of Immunology

<sup>e</sup> McGowan Institute for Regenerative Medicine.

<sup>†</sup> Co-corresponding author.

See DOI: 10.1039/x0xx00000x

10 $\mu\text{m}$  respectively and is reproduced with permission from ref. <sup>12</sup>, Copyright 2008, Nature Publishing Group 2008; Part (B) reproduced with permission from ref. <sup>13</sup>, Copyright 2005, John Wiley and Sons 2005; Part (C) reproduced with permission from ref. <sup>14</sup> Copyright 2014, Nature Publishing Group; Part (D) reproduced with permission from ref. <sup>15</sup> Copyright 2007, Nature Publishing Group; Part (E) reproduced with permission from ref. <sup>16</sup> Copyright 2008, Springer; Part (F) reproduced with permission from ref. <sup>17</sup> Copyright 2011, John Wiley and Sons; Part (G) reproduced with permission from ref. <sup>18</sup> Copyright 2011, John Wiley and Sons; Part (H) reproduced with permission from ref. <sup>19</sup> Copyright 2008, AIP Publishing LLC.

Interestingly, mimicking these macroscopic features is not trivial to accomplish synthetically. Frequently, natural materials assemble in an autonomous fashion through a process known as self-assembly.<sup>20,21</sup> In order to copy this behavior in a lab, researchers have sought to understand the underlying principles governing self-assembling systems with building blocks ranging from proteins to pieces of hot dog.<sup>20–24</sup> For self-assembling systems, the assembly is dictated by the properties of the building blocks and the spontaneous physical and/or chemical interactions that occur among them (with little to no external guidance). The assembly can also be controlled by regulating environmental features, such as the container, charge, and solution in order to determine accessible organizational configurations. The collective characteristics of these building blocks within their environment can be thought of as a set of “directions” for the assembly process. In this way, the size and material composition of the building blocks greatly impacts the organizational complexity of the resulting structure.<sup>24–26</sup> For atomic, molecular, and nanoscale building blocks, self-assembly is a highly accessible fabrication method. Many techniques have been developed to take advantage of natural nano-scale self-assembly with great success, likely due to the strong influence of Brownian motion. However, as the components of a system grow in size, gravity becomes increasingly influential over the components and can overpower Brownian forces, which results in incomplete self-assembly and the development of non-organized materials. Specifically, for systems of spheres, larger “non-Brownian” components ( $d > 6 \mu\text{m}$ ) are more likely to settle into a randomly configured non-equilibrium metastable states, rather than self-assembling into (typically lower energy) crystalline ones.<sup>27</sup> Often for crystallization to occur with macro-sized spherical particles, there must exist a balance between the system’s thermodynamic equilibrium state (being an organized and assembled one) and its kinetics, or the time over which self-assembly can occur.<sup>28</sup> Recently, there have been a number of new studies describing how to induce crystallization via self-assembly among non-Brownian particles to create autonomously forming structures with periodic macroscale features. Unlike their Brownian-influenced counterparts, non-Brownian particles do not naturally self-assemble over an experimentally feasible time-scale; therefore, two generic strategies have been devised for inducing self-assembly: a) elongating the time available for self-assembly to occur or, b) applying an external driver to act as an artificial thermalizing force.<sup>29,30</sup> Equation 1 describes an overestimate for the relaxation time, or the time it takes for a particle to move a distance equal to its own diameter solely due to Brownian motion.

$$(1) T_R = \frac{\eta R^3}{k_B T}$$

Based on this expression where  $k_B$  is the Boltzmann constant,  $T$  is temperature,  $R$  is particle radius, and  $\eta$  is viscosity, it will take a 100  $\mu\text{m}$  polystyrene particle  $10^3$  times longer (over 3 years) to move a distance equal to its diameter than it will take a 1  $\mu\text{m}$  polystyrene particle. In comparison, the time for a 1 $\mu\text{m}$  particle to move 100  $\mu\text{m}$  remains three orders of magnitude faster ( $10^3$  s) than it takes for a

100  $\mu\text{m}$  particle to move that same distance.<sup>29,30</sup> To overcome this time-based limitation (time required for Brownian motion to induce particle motion and subsequently self-assembly leading to crystallization), the most common method for artificially thermalizing a system of non-Brownian particles is through agitation. Adding agitation to a system of particles often leads to enhanced interparticle collisions and interactions in a way that mimics the effects of Brownian motion. For 100  $\mu\text{m}$  particles undergoing agitation (in the form of indirect ultrasonic waves, for example) the time for which self-assembly occurs for a system of particles can be reduced to be on the order of minutes, with the individual particles moving substantially faster as they interact.<sup>30</sup> By analyzing multiple methods to fluidize or artificially thermalize large, non-Brownian particles, many new possibilities arise for adapting current colloidal, micro- and macro-particle organization methods to create new, naturally-inspired materials with macroscopic features for applications that have yet to be explored.

Traditionally, the creation of synthetic materials with macroscopic building blocks has been conducted through top-down methods. In contrast to self-assembly or other bottom-up methods, top down fabrication methods require an external assembler (such as a robot) to drive the assembly based on information stored in a centralized location, such as a blue print. The complexity of the assembled structure stems from the “assemblers” capabilities rather than the building blocks themselves. However, by understanding how to manipulate the building blocks, control over the entire assembly process can be achieved using bottom-up strategies. New routes for bottom-up micro- and nanofabrication as well as a direct path to better design artificial self-assembling systems (albeit synthetically induced) arise from exploring opportunities to expand bottom-up assembly processes to larger building blocks.<sup>20,25,31–33</sup> Manipulating the interactions among individual building blocks leads to method development where precise control over the bulk properties of the resulting material can be obtained. For example, tailoring the building blocks and their orientation, with respect to each other, leads to changes in the overall pore structure (size and distribution) and surface properties (topography, functionalization and area) of a material, which in turn lead to improved regulation over the material’s key functional characteristics such as mechanical strength, diffusive properties, and potentially photonic capabilities.<sup>34–36</sup> The applications of these functional characteristics have the potential to lead to a whole new field of self-assembled, ordered materials on a scale that has been largely untapped to date.

This review will present methods for rationally designing and characterizing materials that exhibit macroscale features and are derived from non-Brownian particles. We describe self-assembly routes for forming macro-crystalline arrays from spherical building blocks that span from the submicron to centimeter scales and that are comprised of materials ranging from gelatin to stainless steel. The versatility of these approaches for manipulating non-Brownian particles have wide appeal for designing novel particle-based materials on all scales.

## 2.0. Fabrication methods for creating crystals from spherical non-Brownian particles

Multiple methods to artificially thermalize and self-assemble large, non-Brownian particles have been developed as a means of fabricating (non-) colloidal crystals with macroscopic features. These methods are largely dependent on an artificial agitation source, manipulating the solvent evaporation rate, customizing the substrate and/or varying the viscosity and cohesiveness of the dispersion medium. Adjusting these environmental parameters in some cases emulates Brownian phenomena and heightens the influence of system thermalization on non-Brownian particles. With respect to particle motion and position adjustability, Brownian particles naturally move erratically through space and explore the physical and energy landscapes before eventually settling. Upon settling, they arrange into a structure which has minimized the free energy of the system. Since non-Brownian particles are not highly influenced by thermal motion, an external stimulus provides this artificial thermalizing force. Particles must have the freedom (as a consequence of the artificial thermalizing energy) to interact with each other and their environment in order to lead to self-assembly. Through these interactions, however, both attractive and repulsive forces influence the organizational state of the crystalline (or non-crystalline) structure formed. Although inter-particle collisions will lead to overall energy dissipation throughout a system of particles, as long as the total energy input to the system is greater than the rate of dissipation, the necessary freedom for erratic and exploratory particle motion is achieved.<sup>20,37,38</sup> Exploring this balance between fluctuational energy (either natural or externally applied) and dissipation has allowed Klotsa and Jack to model the equilibrium dynamics of colloidal systems.<sup>39</sup> Their work describes kinetically trapped states at different time stages throughout the crystallization process and supports the suggestion of Whitesides and Boncheva, describing that particles must be able to adjust their positioning in order to effectively assemble into a periodically ordered structure. Adjustability, or the capability to reverse “incorrect” bonding between particles, avoids kinetic entrapment prior to reaching thermodynamic equilibrium, preventing the development of disorder.<sup>21,28,38</sup> Figure 2 depicts the natural tendency for particles ranging from 548 nm to 1.56 mm to assemble or become kinetically trapped both in the presence and absence of an external agitation source. External agitation is seen to have a substantial impact on the non-Brownian particles (as described in section 2.1.2 and where, in the absence of agitation, kinetic entrapment is seen to occur prior to crystallization. In contrast, in the case of Brownian particles, thermal energy naturally induces particle motion; thus, self-ordering occurs regardless of the externally imposed agitation. For crystallization to occur among non-Brownian particles, constraints on particle size uniformity exist, similarly to those for colloidal particles (coefficient of variation <5%). Additionally, the driving forces behind self-assembly result from varying interparticle interactions when transitioning from the colloidal or Brownian regime to larger non-Brownian particles. The relative influence of forces such as weight (gravity), Van der Waals, electrostatics, and capillary forces changes as the diameter of the particle increases. For larger particles, the influence of weight often dominates. Additionally, mechanical forces derived from interparticle contact can also dictate assembly behavior.<sup>40</sup>

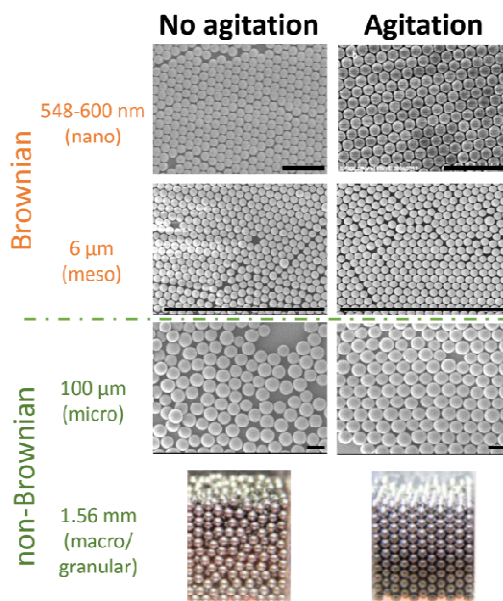


Figure 2: Comparison between nano (scale bar = 5  $\mu\text{m}$ )<sup>30,41</sup>, meso (scale bar = 10  $\mu\text{m}$ )<sup>30</sup>, micro (scale bar = 100  $\mu\text{m}$ )<sup>30</sup> and macro/granular (scale bar = 3 mm)<sup>27</sup> particle packing under gravity and post agitation (organization induced via sonication bath for  $d \leq 100 \mu\text{m}$ , and sinusoidal vibrations for  $d = 1.56 \text{ mm}$ ). Adapted with permission from ref.<sup>30</sup>. Adapted with permission from ref.<sup>30</sup> Copyright 2015, American Chemical Society., ref.<sup>27</sup> Copyright 2008, The American Physical Society. Adapted with permission from ref.<sup>41</sup> Copyright 2006, Elsevier.

Methods for controlling non-Brownian particle assembly can be broken into two large sub-fields in the literature: microparticle assembly and granular assembly. Throughout this review, we will discuss fabrication methods to mobilize and organize uniformly sized spherical particles in both of these size regimes as well as compare the commonalities and differences in these methods and their resulting structures. We will loosely define particle Brownian size ranges as nano ( $700 \text{ nm} > d$ ) and meso ( $800 \text{ nm} < d < 6 \mu\text{m}$ ), and non-Brownian particle size ranges as micro ( $6 \mu\text{m} < d < 900 \mu\text{m}$ ) and macro/granular ( $1000 \mu\text{m} < d$ ) which includes particles with milli- and centimeter dimensions. We acknowledge that the transition between the Brownian and non-Brownian domains is gradual, as Brownian motion is always at play and the gravitational impact scales nonlinearly with particle diameter.<sup>42</sup>

### 2.1. Microparticle assembly for particle-based crystal fabrication

Methods to assemble non-Brownian microparticles have been designed to account for rapid particle sedimentation rates in fluid and the particles' tendency towards kinetic arrest.<sup>30,43</sup> In order to arrange microparticles into crystalline configurations, fluidic forces and solvent evaporation can be controlled and coupled with agitation to increase the time and opportunity for particle interactions.<sup>44,45</sup> The methods described in this review do not focus on those induced using only magnets (albeit effective)<sup>46</sup>, but rather focus on methods that can be applied to a broader set of particle compositions and particle/solvent combinations.

#### 2.1.1. Buoyancy and evaporation induced assembly

## REVIEW

## Soft Matter

Despite the tendency for Brownian forces to have a low impact on larger particle crystallization, these forces can contribute significantly to particle organization when given the proper time and conditions. For example, altering environmental conditions (such as retarding solvent evaporation, adding thermal energy, and density matching the solvent and particle) can minimize the influence of gravity and enhance the impact of the interparticle interactions governing the overall particle behavior. Two methods to achieve this balance between particle buoyancy and evaporation have been reported in the literature and are summarized below. The first is a Mixed Solvent Evaporation method. This process is carried out with 75  $\mu\text{m}$  polystyrene particles in a 3:1 water: dimethylformamide (DMF) solvent. The balance between the solvent evaporation rate and buoyancy allow for enhanced time prior to particle sedimentation which promotes particle movement and interactions. This Mixed Solvent Evaporation method leads to solvent-free crystals forming over the course of days without the need for external agitation. DMF was chosen for being a polar organic solvent with a higher boiling point than water and a density similar to that of polystyrene and water.<sup>47</sup> Based on a similar principle of balancing particle and solvent density, an alternative, or second approach is a floating route to self-assembly. This approach has been applied to a system of polystyrene particles ranging in size from 10–240  $\mu\text{m}$  in ethylene glycol at 100 °C in a slightly porous, covered vial. In this floating assembly method, the particles are influenced by a combination of buoyancy, gravity, electrostatics (attractive and repulsive) and lateral capillary forces (floating and immersion). The combination of these forces allows the particles to move and adjust their positioning as they ascend and self-organize at the fluid surface, leaving a particle-based crystal to be recovered upon complete solvent evaporation.<sup>48</sup>

### 2.1.2. Sonication induced assembly

Many groups have employed a sonication bath as a means of agitating particles through an external (non-thermodynamic) energy source. Within a sonication bath, ultrasonic waves emanate from the bath, causing pressure differences within the bath fluid (usually water) resulting in the formation of cavitation bubbles.<sup>49</sup> By altering the bath medium, the impact of the ultrasonic waves and resulting fluid agitation may be altered and in turn alter particle motion.<sup>30</sup> Kotov and coworkers have shown that exposing large soda lime, polystyrene, or PMMA microparticles (ranging in size from 75–160  $\mu\text{m}$ ) to a slowly evaporating solvent and introducing gentle ultrasonic energy over time leads to the formation of high quality three-dimensional crystalline structures. A solution of particles is slowly added to a vial set on top of a sonication bath cover for exposure to gentle agitation. In this way, direct contact with the bath as a strong agitation source is avoided and only mild agitation is felt by the sample as the particles sediment. After full sedimentation, the sample is removed from the sonication bath and solvent evaporation is allowed to occur over a few days' time.<sup>50–54</sup>

More recently, a method has been developed for making both two- and three-dimensional crystals using sonication as an energy input source for particles ranging from the nanoscale up to sub-millimeter scale with 750  $\mu\text{m}$  particles. In these studies, monodispersed particles made from either polystyrene or soda lime disperse in

deionized water (10% w/v) on a variety of substrates and are exposed directly to ultrasonic agitation at varying energy inputs.<sup>30</sup> Their results suggest that this process can be extended to mixtures for the production of multicomponent crystals. This method successfully organizes particles on both flat substrates as well as in glass vials and conical plastic containers. The crystallization process is a function of interparticle interactions induced by the sonication input and not a function of solvent evaporation.<sup>30,55</sup> However, fluid evaporation is the time limiting factor in all of these sonication-induced processes.

### 2.1.3. Shaking induced assembly

Several reports also show a method for creating close-packed crystals through orbital or reciprocating shaking. Choi et al. create a cubic close packed (CCP) lattice of poly( $\epsilon$ -caprolactone) (PCL) microparticles by exposing a well-mixed, low density particle solution to continuous orbital shaking at 80 rpm throughout the solvent evaporation process.<sup>56</sup> To adapt this method to multiple different types of particles (material compositions) including gelatin, they also add a brief tapping component to their fabrication process.<sup>57</sup> Additionally, Stachowiak et al. report the assembly of poly(methyl methacrylate) (PMMA) spheres at a high density (40–65% w/v) solution in 70% ethanol at 250 rpm and 20 °C on a reciprocating shaker until complete solvent evaporation is achieved. They report that subsequent steps of wetting and shaking may be necessary for an ordered crystal to form.<sup>58,59</sup>

### 2.1.4. Vibrational Compacting (tapping) induced assembly

Similar to the shaking induced assembly of microparticles, a mechanical agitation source in the form of tapping applied to a sample can lead to three-dimensional particle assembly. Choi et al. present a method for large microparticle crystallization based on substrate geometry and a controlled solvent evaporation rate. Their vertical tapping method was performed on a concave glass dish. Gelatin spheres were allowed time to settle into a randomly packed state and upon vertical tapping on the glass, a periodic, close-packed lattice formed.<sup>43</sup> This tapping method was then modified such that it could be carried out in a plastic centrifuge tube to produce a three-dimensional crystal and in a rectangular mold (at an angle) to produce a two-dimensional crystal. Under these modified conditions, periodic close-packed crystals formed from gentle tapping on the sides of the container during the solvent evaporation process.<sup>45,60</sup>

### 2.2. Granular-particle assembly for particle-based crystal fabrication

Packing granular particles has been widely researched across the literature to study the packing density of particles and powders and their subsequent phase behavior. For example, particles of a variety of material compositions, including glass and metal, have been transformed from a granular gaseous phase to a crystalline one by tuning the vibration applied to the holding container in clever ways. In granular packing, gravity, granular temperature, and energy dissipation are essential variables in determining the crystalline (or non-crystalline) configuration.<sup>61,62</sup> In contrast to the methods described above for microparticles, most granular assembly methods are applied to dry or slightly saturated particle beds, rather than particles submerged in fluid.<sup>27,61,63–66</sup> In the absence of a

solvent, there is a change in influential interparticle interactions, resulting in different particle behavior. However, despite this difference, the need for an external energy input to influence self-assembly remains constant. These assembly methods are based on energy dissipation and mechanical vibrations and can be broken into two large groups: those aimed at crystallizing a disordered bed of particles and those aimed at creating a crystal through epitaxial (particle-by particle and layer-by-layer) methods.<sup>27,61,64</sup> These two overarching fabrication routes have been largely studied for both dry and cohesive systems under vibrational annealing.<sup>27</sup>

### 2.2.1. Vibration induced assembly of a randomly packed particles

When added to a container and under the influence of gravity, particles tend to organize with a packing density of  $\rho \approx 0.6$  into a random configuration. However, by adding vibrations in one (vertical), two (horizontal), and three dimensions (vertical plus horizontal), a slight transformation occurs to increase packing density.<sup>67,68</sup> By tuning the vertical vibrations for a system of stainless-steel beads, Urbach and Olafson created a two dimensional organized layer of particles via vibrational energy imparted to encourage particle-particle collisions. Their studies were among the first to organize granular particles and study the effects of the collision rate (with variables dependent on vibration frequency and amplitude) on the resulting structural order.<sup>66</sup>

However,  $\rho = 0.6$  is not the upper bound for a three-dimensional granular packing density. By introducing vertical vibration into the system of particles, the packing density can be increased up to  $\rho = 0.64$ , or to a randomly close packed (RCP) configuration.<sup>67</sup> Adding a horizontal or a combination of vertical and horizontal vibrations further increases the packing density to  $\rho = 0.655$  and  $0.661$ , respectively.<sup>67</sup> The impact of three-dimensional vibrations on glass particle packing was further analyzed by Li et al. where their studies show the effects of packing density over time as a function of the vibrational frequency and amplitude. They found that packing density initially increases with vibration amplitude or frequency to a maximum value and then either plateaus or decreases after a certain time period.<sup>68</sup> This upper bound on the packing density is likely due to jamming and is hard to overcome without batch-wise or continuous addition of particles during the vibrational process.<sup>67</sup>

### 2.2.2. Epitaxial crystal growth

Epitaxial techniques use gravity to create ordered, granular crystals in a piece-wise fashion. The growth is largely governed by particle sedimentation, and is highly dependent on the substrate and suspension properties.<sup>62</sup> Many approaches are based on slow sedimentation of hard spheres, and investigate the effects of varying vibrational amplitude and frequency in all dimensions.<sup>61,67</sup>

Pouliquen et al. describe one of the first reports to create crystals from granular glass beads by employing horizontal agitation forces. Their setup is designed to mimic colloidal behavior among non-Brownian particles by introducing chaos into the system via particle-bar collisions during the filling process. They achieve this level of chaos by holding a funnel over horizontal cylindrical bars above a rectangular container, where the arrangement of the bars increases the inter-particle collision rate, and leads to the creation of a more homogeneous distribution of particles. Throughout this

process, the container undergoes horizontal vibration and results in the formation of close packed structures. By altering the particle deposition speed and boundary conditions (container size/shape) in relation to particle size, they are able to rationally create large face centered cubic (FCC) and hexagonally close packed (HCP) regions throughout the crystal as well as square packed regions at the free surface.<sup>69</sup> Nahmad-Molinari and Ruiz-Suárez later show that defect free HCP crystals can form in triangular containers by controlling the rate at which steel ball bearings are added and exposed to vertical vibrations. In their experiments, particles are added one by one at a given, controlled frequency. Through this slow, yet continuous addition process, they demonstrate the relationship between energy dissipation among the particles and the self-stabilization of seed clusters growing into larger crystalline domains.<sup>61</sup>

More recently, Panaitescu and Kudrolli have shown that vibrations are not crucial to the assembly process if a patterned substrate is used in conjunction with a highly controlled particle sedimentation rate. In their studies, gravitational sedimentation can act as the driving force towards crystallization of plastic particles if the deposition rate of particles onto the substrate is sufficiently slow. As the particles individually drop onto the patterned substrate in a continuous fashion, they must independently come to rest, one at a time, without damaging the substrate to produce an ordered structure. If one particle dislodges another particle, the whole particle bed is likely to become disordered. Therefore, tweaking the deposition conditions, the phase state of a packed bed, can be transformed between crystalline (ordered) and amorphous (disordered) states.<sup>64</sup>

The growth of crystals through epitaxial methods is not restricted to a single particle being continuously added over time. Many groups have shown that a batch-wise addition works well to achieve FCC and HCP configurations.<sup>67,68,70</sup> Yu et al. show experiment and through simulation that the size of the batch (the number of particles added at a given time) coupled with the vibrational characteristics (frequency and amplitude) has a substantial impact on the crystallization process. Their results suggest that the number of particles added per batch should be equal to the number of particles necessary to fill one complete layer within a given container in order to achieve the densest packing.<sup>67</sup>

## 3.0. Characteristics of non-Brownian particle-based crystals

The characteristics of a crystal, or its form, can directly dictate its functionality as a material. Similar to the Brownian particle self-assembly literature, the non-Brownian particle literature has established ways to characterize crystal quality through the particle packing density, appearance of defects and grain boundaries, and the overall particle coordination or order parameter.

### 3.1. Packing density as a function of the crystal fabrication method

Through the aforementioned fabrication methods, a great number of different organizational configurations, with varying packing densities and stabilities, can be formed.<sup>67,71,72</sup> The Hales proof of the Kepler conjecture illustrates that for perfect hard spheres, the

## REVIEW

## Soft Matter

highest packing density achievable is  $\rho=0.74$ .<sup>71,72</sup> For spherical particles, natural thermalizing forces will naturally draw the components together with a packing density of  $0.6 < \rho < 0.64$ , or into a random close packed way.<sup>73,74</sup> When agitation in a single direction is added, a randomly close packed arrangement with  $\rho=0.64$  repeatedly forms, and with more dynamic vibration (three-dimensional), a close packed structure with  $0.68 < \rho < 0.74$  develops.<sup>67</sup>

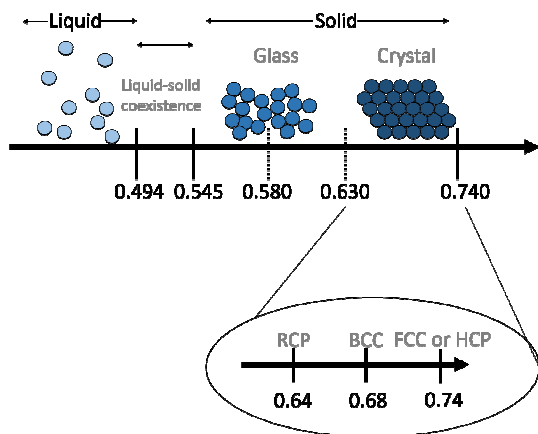


Figure 3: Variation in the particle packing density leads to changes in the phase behaviour of a system of particles. The transitions between liquid and crystalline phases for three-dimensional spherical particle systems can be observed for densities ranging from below 0.494 up to 0.74.<sup>62,75,76</sup>

Many methods seek to produce high-density crystals with either HCP or FCC arrangements. From a packing density and thermodynamic viewpoint, these two packing configurations are similar, but from a force dynamics and elasticity perspective, they differ greatly.<sup>77,78</sup> In an FCC structure, each particle is supported by the three particles directly below it. The direct line of contact among the particles is straight and spans the length of the structure. Therefore, when a force is applied to the crystal, it is transmitted in a straight line from particle to particle, forming a triangular pattern at the bottom surface. Conversely, in an HCP structure, the particle-particle contact line does not exist in the form of a continuous straight line. In the HCP arrangement the contact line zigzags, causing the force to be divided across every other layer, resulting in a ring of maximum force.<sup>77</sup>

To deliberately create a packed structure of a certain orientation, strategic utilization of the container shape (triangular, rectangular, cylindrical) and environment can be influential and even predictive in governing the resulting organizational configuration.<sup>63</sup> For example, a triangular container will inhibit the ideal formation of an FCC crystal and a square container will inhibit the formation of an ideal HCP crystal.<sup>27</sup> However, a triangular container can act to promote condensation of an HCP structure.<sup>61</sup> Forming a specific crystal orientation in the improper geometric constraints will lead to the development of defects or grain boundaries throughout the bulk crystal. Furthermore, Carvente et al. report that changing the saturation within the environment (in addition to container shape) impacts the orientation. Their findings suggest that dry, granular particles in a rectangular container can be coerced to self-assemble into a BCT structure, while cohesive beads form FCC crystals. They conduct this study and make the conformational changes noted by

adding defined amounts of oil to their system to tweak the organizational structure right before the system undergoes vibrational annealing. The formation of liquid bridges between the particles alters the interparticle interactions due to the introduction of capillary forces and helps induce different crystalline orientations.<sup>27,37</sup>

Similarly to the open systems we have primarily discussed, adjusting the container properties appropriately also provides design control over the resulting crystal orientation when creating crystals in a closed system (where the particles are added to the container prior to vibrational annealing).<sup>27,63</sup> Low ratios of the container diameter to particle diameter have been shown to induce crystallization and increase the overall packing fraction.<sup>79</sup> Organizing particles in narrow containers, for instance, forces the particles to pack in planes parallel to the walls, leading to the formation of body centered tetragonal (BCT) orientations. As the space between the walls increases, the impact of shearing slowly diminishes, and gravity forces the rotation of the plane orientation yielding a diagonal FCC structure (pending that the crystal domain fits within the dimensions of the container).<sup>63</sup>

Studies have shown that when exposed to any type of vibration, the packing density of a particle bed will first increase to a maxima, and then plateau or slightly diminish over time. This trend is observed for granular beads both transforming from of a randomly packed particle bed to a crystalline state as well as for those being batch wise added to a particle bed.<sup>67,68</sup> Furthermore, the packing density can be controlled by independently controlling the vibrational amplitude and frequency for crystals produced from both epitaxial and non-epitaxial crystal growth methods.<sup>68</sup> At both low and high frequency and amplitude, the packing fraction remains lower than RCP. Its behavior between these limits is parabolic, showing a maximum at a mid-range for both parameters. Additionally, creating a batch-wise or slow particle addition process aids in the process of increasing packing density, trending towards a higher density corresponding to fewer particles per batch, and more batches.<sup>64,68,69</sup>

### 3.2. Defect development

Colloidal crystals produced via self-assembly consistently form with defects intrinsically embedded within their structure. These defects can be classified into two categories: macro- defects (growth bands and cracks) and micro- defects (vacancies and stacking faults).<sup>80,81</sup> On the nanoscale, defects such as cracks have been shown to form during the solvent evaporation process (due to tensile stress buildup) as the crystal shrinks.<sup>81,82</sup> The formation of a crack is more likely to emerge between hard spheres (as compared to soft spheres) as a method of alleviating built up stress; furthermore, it was found that cracks tend to develop in the direction of the evaporating fluid.<sup>83,84</sup> While a great deal of research has been done among nanoparticles to overcome the challenges associated with defect formation, (such as tuning the particle interaction potential in solution and the drying rate) minimal research has been done to study this phenomenon among non-Brownian particles.<sup>81,85</sup> For the microparticle assembly fabrication methods described in Section 2 that rely on crystallization occurring prior to complete solvent evaporation, we hypothesize that large microparticle-based crystals

undergo similar shrinkage and therefore succumb to a similar process of crack formation. The epitaxial granular crystallization methods, however, are often used in systems containing dry particles or slightly damp particles; therefore, they succumb to different interparticle interaction forces and are not as susceptible to crack and defect formation.<sup>61</sup> Nevertheless, defects and polycrystalline states can still form. Increasing the time allowed for the particles to adjust their position before jamming or becoming arrested in place (i.e. through slower particle addition to the particle bed) allows for the dissolution of these defects, resulting in an improved crystalline structure.<sup>61</sup> For this reason, granular crystals, unlike micro- and nano- particle-based crystals, are often grown to be defect-free. In granular distributions, point defects and faults can be created or removed manually by adding/removing a particle or switching the plane orientation between FCC and HCP during an epitaxial (layer-by-layer) growth process.<sup>27,61,63,86</sup>

There is a large body of literature studying the growth process and lasting effects of defects and impurities within crystalline structures. One of the biggest impacts that defects have on the function of a particle-based crystal comes from a change in the overall packing density, which in turn causes a change in the way that force propagates through the structure (as described in Section 3.1).<sup>67,86</sup> Based off of techniques to reduce defects over the entire body of self-assembly induced crystallization literature, precisely controlling the particle environment leads to higher quality crystals forming. For non-Brownian particles, properly sizing the container with respect to the particle diameter can impact the presence (or absence) of defect formation. Additionally with micro- and milliparticles, it has been shown that increasing the intensity of the agitation (to a degree) can also help to reduce the presence of defects.<sup>30,67</sup>

### 3.3. Complex and hierarchical packing structures

Monodispersed, particle-based crystals can be altered to exhibit hierarchical features at the macro, micro- and nano-scales.<sup>87</sup> Adding hierarchy and complexity within a crystal creates the opportunity to form higher density materials as well as control the interparticle spacing between the largest particles. By altering the density and packing orientation of the particles in the crystal, the line of force propagation through the material changes, altering the material's capacity to withstand functional stress and strain.<sup>77,88</sup> Specifically, by incorporating size heterogeneity into the building blocks increases its uses as a templating material.<sup>9</sup> By having multiple different component building blocks, environmental cues and information can be encoded into the structure for different applications, like biological ones that direct cellular migration or enhance the material's load-bearing capabilities.<sup>6,9,89,90</sup> As a template, the material can be used to form imprints for surface patterning or as a substrate or mold for further material creation.<sup>9,87</sup> In the creation of porous materials, hierarchical or complex particle-based crystals may also simultaneously exploit the advantages provided by multiple pore sizes and increase the available surface area and pore volume of a material. Nano- and micro-sized pores can be combined to create ample reactive sites and interfacial area for reactions to occur as well as provide size-selectivity in filtration. By further combining nano- and micro-sized pores with larger macro-sized pores, mass transport through the

structure can be drastically improved by reducing transport limitations innate to singularly smaller pores or a lack of interconnectivity.<sup>91</sup>

Historically, multicomponent crystals have been solely produced from colloidal, or nanoparticles.<sup>92-94</sup> Recently, however, binary and multicomponent crystals have been created from completely non-Brownian particle mixtures.<sup>55</sup> These multicomponent crystals are produced in a sonication bath similarly to those described in Section 2.1.2, where polystyrene and soda lime particle mixtures are dispersed in water are exposed to ultrasonic energy in order to organize over time. Like their nanoparticle counterparts, mixtures of non-Brownian microparticles can organize into a variety of configurations by varying the number and size ratios of the particles in the mixture, just as seen in the production of stoichiometric-like structures (or patterns) that mimic those formed by atoms. However, these types of configurations have not yet been achieved among granular beads. By creating these stoichiometric structures from larger, synthetic particles, new routes for studying interesting atomic and molecular behavior become more readily available.<sup>55,92,93,95</sup> Specifically, varying the number of small (S) to large (L) particles in a binary mixture, or small to medium to large particles within a ternary mixture, allows for a variety of mimetic structures to be created, including those that structurally resemble molecules like NaSe<sub>8</sub>, AuCu<sub>3</sub>, AlB<sub>2</sub>, NaCl, ZnS, AlMgB<sub>3</sub>, AuCsCl<sub>3</sub>, etc. as seen in Figure 4.<sup>92,95,96</sup>

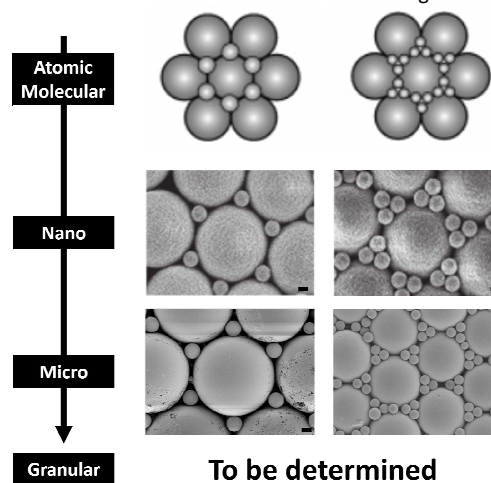


Figure 4: Stoichiometric particle assemblies on the nano-<sup>97</sup> and micro-scales<sup>55</sup> mimicking structures naturally formed on the atomic and molecular scales<sup>98</sup> with LS<sub>2</sub> and LS<sub>6</sub> or LS<sub>8</sub> configurations. On the nanoscale organization was promoted via interfacial assembly at an air-water interface and on the micro scale via a sonication bath. These types of orientations are theoretically possible on the granular scale but have yet to be created. Adapted with permission from ref.<sup>98</sup> Copyright 2015, American Chemical Society, ref.<sup>97</sup> Copyright 2011, John Wiley and Sons, ref.<sup>55</sup> permissions still needed from John Wiley and Sons.

### 4.0. Characterization of crystallinity

A multitude of order parameters to assess colloidal crystal quality have been developed and validated throughout the literature. In the simplest terms, these order parameters measure how many hard sphere particles are in a given crystalline domain and the orientation of these particles with respect to their neighbors.



## REVIEW

## Soft Matter

In a two dimensional area of dense particles, the Mermin order parameter can be computed by a sum over the nearest neighbors for a particle at a given position,  $r$ , at an angle of  $\theta$ .<sup>99</sup> This relationship can be described by:

$$(2) \quad \Psi_6(r) = \frac{1}{N_b} \sum_k \exp(i6\theta_k) \text{ where } k = 1, \dots, N_b$$

In the case of HCP or FCC crystalline packing, this computation can be simplified. Knowing that a fully coordinated particle will have six neighbors, the distance between these six pairs of particles/neighbors can be quantified to determine regularity and order through the magnitude of the measured standard deviation (low values correspond to a higher degree of order). Additionally, quantifying the coordination of each particle with respect to its neighbors and each neighbor's coordination over a given area, the packing density and crystalline quality can be described.<sup>30</sup> While these methods work well for two-dimensional crystals (or two-dimensional representations of three-dimensional crystals) made from non-colloidal particles, more accurate measurements in three dimensions become more computationally extensive.<sup>30,100,101</sup>

Three-dimensional hard sphere dense packing orientations can be described by the commonly used Steinhardt, tetrahedral, or nematic order parameters and have been done so extensively in the literature for colloidal crystals. In practice, these types of orientational order parameters (which account for particle coordination) are combined with a translational order parameter (which accounts for the radial distribution function) to describe densely packed particle systems at equilibrium and throughout their process to get there.<sup>74,99</sup> When combining the Steinhardt order parameter with the translational order parameter, a positive correlation emerges for hard sphere systems, revealing descriptive information for systems ranging from jammed states to those in complete disorder to those that are ordered crystals.<sup>74,102,103</sup> The bond orientational order parameter has been shown to accurately describe glassy structures as not purely liquid-like, but rather describes their intermediate states ranging between the liquid and crystal phases.<sup>74,99</sup>

Experimentally, with large amounts of microparticles or a collection of granular particles (due to their large size) it is also common to measure the average volume or packing fraction through measurements of height and weight (or number of particles) of the packed particle bed.<sup>68,69</sup> In this method, the measurements are fast and easy and can show distinct differences between RCP and FCC/HCP systems.<sup>61,104,105</sup>

### 5.0.Applications of non-Brownian particle-based crystals and their inverted structures

Crystals produced from non-Brownian particles offer different advantages to those produced from Brownian particles.<sup>33</sup> While many of the applications of non-Brownian particles may have overlap with the Brownian regime, a distinct advantage to working with larger particles is simplicity and ease of production and characterization. Since larger building blocks are easier to produce and visually easier to track (with and without a microscope),

improved monitoring of the overall the crystallization process can be achieved. Larger components also provide more user control in the crystallization process (compared to molecules and nanoparticles) in terms of the strength, range and selectivity of the interparticle interactions.<sup>25,26</sup> By inducing self-assembly to organize non-Brownian particles for macroscale materials design, as described throughout this review, the complexity of the material structure can be determined by the building blocks (as a sort of encoded information) rather than by the limitations set forth by the assembler in a top-down assembly process. Advances in non-Brownian particle science make bottom-up assembly a reality for a new regime of building blocks capable of producing metamaterials as well as those with naturally-inspired architectures via cost and time-efficient processes.<sup>33,38</sup>

Additionally, materials with larger pores (as compared to those made from colloids) and structural features are particularly useful for the production of photonic and phononic materials,<sup>36,93,106,107</sup> templating and patterning biological substrates,<sup>108</sup> drug delivery, microelectronics,<sup>25</sup> catalysis,<sup>35,109</sup> filtration, and as model systems to study stress propagation.<sup>63,77</sup> Understanding the behavior of large components, such as millimeter-sized particles, as they crystallize or form densely packed structures can be used in the study of granular flow where crystallization would lead to jamming and complications in industrial production processes.<sup>63,73,110-112</sup> Further investigation into the packing of non-spherical non-Brownian particles can also lead to the creation of more densely packed structures with wide implications in consumer products and packaging, as in the economically relevant problem of how much grain can fit into a barrel.<sup>72,73</sup> For example, Donev et al. demonstrate higher packing fractions for ellipsoid-shaped M&M's, reaching a random packing density approaching  $\rho=0.74$ , as compared to  $\rho=0.64$  for RCP spheres.<sup>73</sup> The implications of this work spread beyond the science of M&M's and can be translated industrially for ellipsoids with varying dimensions and material compositions. The underlying physical science driving non-Brownian particle behavior can also be useful in explaining natural phenomena, such as the clotting of blood cells. While a cell is not spherical like the building blocks discussed throughout this review, understanding the forces and interactions acting upon larger components in a variety of environments can bring new insight to important biological processes.<sup>113</sup> For instance, understanding the clotting (or aggregation) phenomena of these cells in terms of their physical interactions may help to both promote clotting in wound healing as well as prevent clotting and the associated adverse side effects from clotting-induced ailments (deep vein thrombosis, heart attack, stroke, etc.).<sup>113</sup>

In addition to its uses in manipulating packing density and aggregation, understanding non-Brownian particle behavior leads to the creation of sophisticated templating materials. Non-Brownian particle-based crystals and their inverse structures have created a new subfield of interconnected and readily reproducible scaffolds that are being widely investigated for regenerative medicine applications. Numerous studies have shown enhanced transport of nutrients as well as cellular infiltration throughout inverted crystalline (ICC) scaffolds, for bone and cartilage regeneration in addition to *ex vivo* spheroid production for liver

cells.<sup>51,57,114–118</sup> These scaffolds have been made from materials such as poly(2-hydroxyethyl methacrylate) (pHEMA), polyacrylamide hydrogels, poly(lactic-co-glycolic acid) (PLGA), chitosan, and tricalcium phosphate cement as well as combinations of various other polymer blends from assembly methods described throughout Section 2.<sup>56,115,119,120</sup> It has been shown that with a biocompatible material, scaffolds with this type of uniform, interconnected pore architecture, can improve vascularization and ultimately enhance tissue regeneration.<sup>121</sup> Various studies have explored changing both the scaffolding material and the particle size and fusion conditions to control the various pore sizes within the matrix (including surface pores, windows, and internal pores).<sup>114,119,122</sup> By altering the composition and pore structure, or form, of the scaffold, the function of the scaffold can be tailored to treat ailments ranging from filling bone defects to replacing damaged alveolar (lung) tissue. ICC's currently show great potential as regenerative therapies, yet there still lies unanswered questions regarding optimal structures for various tissue engineering challenges.<sup>114,115</sup> Further research into the effects that different mechanical and surface properties have on various cell types (as well as how the bioactivity and degradation profile of a material impacts cellular behavior in the tissue building process) will help to better establish inverted crystals as a translational regenerative therapy.

In the future, these types of hierarchical materials will likely expand in utilization into the energy fields for applications including adsorbents, catalyst supports, electrodes for batteries, double layer capacitors, and host sites for hydrogen storage.<sup>4,34,35,91</sup> Specifically, porous carbon is a popular platform material for these applications due to its chemical inertness and thermal stability. As a base material for fuel cell electrodes, ICC structures offer functional benefits in the creation of high surface area, thin walls and high degrees of customizability and reproducibility. Bicontinuous structures of this sort provide an open, continuous pore space which is favorable for electrolyte access and continuous walls which aid in the conduction of electrons and ions. By creating structures with large surface availability, there are more sites for charge transfer across the electrolyte/electrode interface, potentially creating a more efficient electrode material.<sup>4,35,91</sup>

A great deal of research has explored inverted crystals in this way produces from Brownian particles on the nano- scale but limited studies have investigated the potential of non-Brownian particle derived structures. Using non-Brownian particles as a template for creating new ICC-based hierarchical materials may provide enhanced structural functionality, larger pores for mass transport and greater surface availability than current technologies can.<sup>4,35</sup>

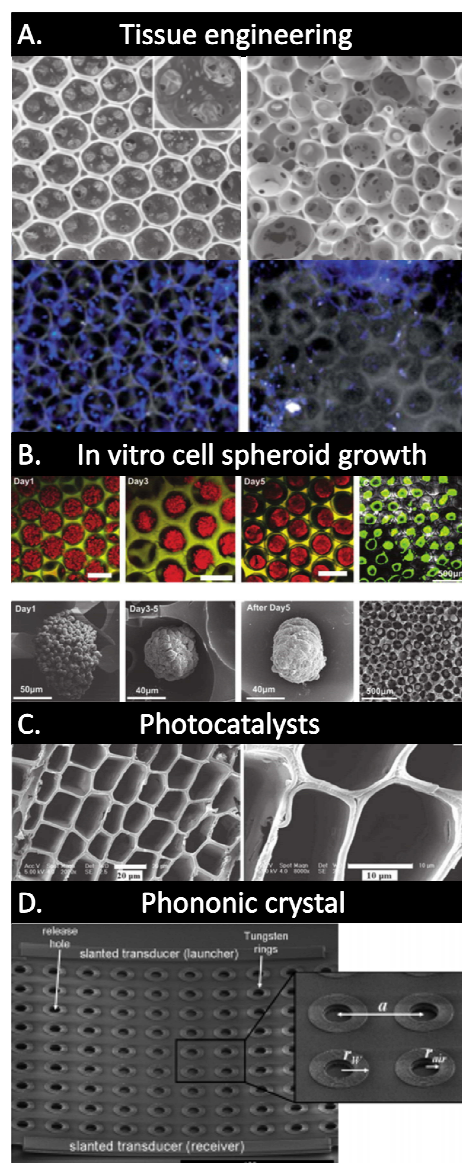


Figure 5: Examples of using macro-features to enhance the function of materials ranging with application from tissue engineering to phononics. A) Tissue engineering scaffold produced from PLGA. The SEM and fluorescence micrographs illustrate scaffold organization and interconnectivity with fibroblast (DAPI staining) penetration through the organized ICC scaffold produced as in Section 2.1.4 (pore size = 211 $\mu$ m) on the left hand side in a better way than the un-organized scaffold on the right hand side. B) ICC scaffolds produced as in Section 2.1.2 used to produce cell spheroids ex vivo. C) Cedar wood coated in TiO<sub>2</sub> for photocatalysis. D) SEM of a W-in-SiO<sub>2</sub> Phononic Crystal. Part (A) Reproduced with permission from ref<sup>123</sup> Copyright 2010, American Chemical Society; Part (B) Reproduced with permission from ref<sup>116</sup> Copyright 2009, Elsevier; Part (C) Reproduced with permission from ref<sup>124</sup> Copyright 2009, Springer; Part (D) Reproduced with permission from ref<sup>125</sup> Copyright 2010, AIP Publishing LLC.

## 6.0. Conclusion and perspective on translation from bench-top to industrial use

The nascent field of non-Brownian particle self-assembly has grown substantially in the past five to ten years with applications of porous materials, ranging from regenerative medicine to photonics, to tackling the age-old problem of granular compaction. There still exists a breach in the literature, however, between micron and granular-scale science. A large majority of research for both

## REVIEW

## Soft Matter

microparticle and granular particle systems shows that crystallization occurs as a result of agitation; however the microparticle literature mainly studies wet systems while the granular literature studies mainly dry systems. Additionally, when looking at multicomponent mixtures, the microparticle literature just recently expanded to include studies of co-crystallization to create stoichiometry-mimetic structures in much the same way the nanoparticle literature has done. Granular particle mixtures, however, generally are studied for how they mix and segregate and have not been extended in this way to mimic atomic behavior.<sup>126,127</sup>

By studying both wet and dry particle systems across size scales, there lies potential for extending the science behind particle rearrangement to rationally design structures with specific macro-, micro-, and nano- architectures.

Bridging these fields even more in practice will further elucidate interparticle phenomena in a practical and scalable way that can have a significant impact on understanding crystallization at larger scales. For instance, extending the methods leading to spherical non-Brownian particle crystallization on a bench scale can be scaled to create larger crystalline domains as well as to create methods applicable for systems of non-spherical building blocks. Additionally, this type of understanding can be applied to designing precise packing configurations and achieving desired crystal orientations. Deliberate crystal growth of this kind has the potential to lead to the creation of structures with a variety of functions stemming from different (and customizable) physical properties including mechanical stiffness, structural density, and mass transport potential (derived from the pore size and pore size distribution). Investigating particle behavior at the macro-scale as an extension of what has been thoroughly studied on the nano-scale creates new possibilities for translation of the fundamental science into scalable fabrication methods. Traditionally top-down, assembler-based, fabrication methods have been solely used for assembling large particles since self-assembly of non-Brownian particles has not been developed on an industrial scale.<sup>24,25,128</sup> However, with the increase in knowledge of non-Brownian particle interactions and assembly, this challenge can be overcome to produce uniquely porous materials, featuring complex structures with customizable surface functionalization and multi-scale hierarchy. Exploration into the fabrication and application of non-Brownian particle-based crystals has the potential to transform biomedicine through ICC scaffold creation, enhance the efficiency of ion transport in battery-based materials through high surface area, more precisely filter sound waves for phononics as well as transform the state of the art in a plethora of undiscovered applications to improve human life.

### Acknowledgements

ML was supported by the University of Pittsburgh's Provosts Development Fund and the U.S. Dept. of Ed. GAANN PR/Award No: P200A100087.

### Notes and references

‡ The term inverted colloidal crystal (ICC) used in this paper is a convention used throughout the literature to represent an inverted crystalline structure produced from particles both in and out of the "colloidal" size range.

§ ref 55 has been accepted but is not yet in print.

- 1 Z. Tang, N. A. Kotov, S. Magonov and B. Ozturk, *Nat. Mater.*, 2003, **2**, 413–418.
- 2 K. S. Katti, B. Mohanty and D. R. Katti, *J. Mater. Res.*, 2006, **21**, 1237–1242.
- 3 Z. Huang, Z. Pan, H. Li, Q. Wei and X. Li, *J. Mater. Res.*, 2014, **29**, 1573–1578.
- 4 Y. Li, Z.-Y. Fu and B.-L. Su, *Adv. Funct. Mater.*, 2012, **22**, 4634–4667.
- 5 R. Lakes, *Nature*, 1993, **361**, 511–515.
- 6 S. Bechtler, S. F. Ang and G. A. Schneider, *Biomaterials*, 2010, **31**, 6378–85.
- 7 T. Sano and C. L. Rando, *JOM*, 2012, **64**, 212–213.
- 8 Z. Zhang, Y.-W. Zhang and H. Gao, *Proc. Biol. Sci.*, 2011, **278**, 519–25.
- 9 A. Wang, J. Huang and Y. Yan, *Soft Matter*, 2014, **10**, 3362–73.
- 10 R. C. Hardie, *Curr. Biol.*, 2012, **22**, R12–R14.
- 11 M. Friedrich, *Integr. Comp. Biol.*, 2003, **43**, 508–21.
- 12 J. Lim, J. Crespo-Barreto, P. Jafar-Nejad, A. B. Bowman, R. Richman, D. E. Hill, H. T. Orr and H. Y. Zoghbi, *Nature*, 2008, **452**, 713–718.
- 13 J. P. Li, S. H. Li, C. a Van Blitterswijk and K. de Groot, *J. Biomed. Mater. Res. A*, 2005, **73**, 223–233.
- 14 I. Solomonov, D. Talmi-Frank, Y. Milstein, S. Addadi, A. Aleshin and I. Sagi, *Sci. Rep.*, 2014, **4**, 1–7.
- 15 P. Ball, *Nature*, 2007, **449**, 10–11.
- 16 F. H. Kaatz, A. Bultheel and T. Egami, *Naturwissenschaften*, 2008, **95**, 1033–1040.
- 17 R. M. L. Guimarães, B. C. Ball and C. a. Tormena, *Soil Use Manag.*, 2011, **27**, 395–403.
- 18 P. Ball, *Archit. Des.*, 2012, **82**, 22–27.
- 19 Z. Guo, W. Liu and B. L. Su, *Appl. Phys. Lett.*, 2008, **93**.
- 20 G. M. Whitesides and B. A. Grzybowski, *Science*, 2002, **295**, 2418–21.
- 21 R. L. Jack, M. F. Hagan and D. Chandler, *Phys. Rev. E - Stat. Nonlinear, Soft Matter Phys.*, 2007, **76**, 1–8.

## Soft Matter

## REVIEW

- 22 D. J. Campbell, E. R. Freidinger, J. M. Hastings and M. K. Querns, *J. Chem. Educ.*, 2002, **79**, 201.
- 23 B. Sweeney, T. Zhang and R. Schwartz, *Biophys. J.*, 2008, **94**, 772–83.
- 24 L. Cademartiri and K. J. M. Bishop, *Nat. Mater.*, 2014, **14**, 2–9.
- 25 M. Boncheva, D. Bruzewicz and G. M. Whitesides, *Pure Appl. Chem.*, 2003, **75**, 621–630.
- 26 B. R. Groq and M. Dorigo, *Proc. IEEE*, 2008, **96**, 1490–1508.
- 27 O. Carvente and J. Ruiz-Suárez, *Phys. Rev. E*, 2008, **78**, 011302.
- 28 D. Klotsa and R. L. Jack, *Soft Matter*, 2011, **7**, 6294–6303.
- 29 P. N. Poon, W.C.K.; Pusey, *Obs. Predict. Simul. phase transitions complex fluids*, 1995, 3–51.
- 30 M. H. Lash, M. V. Fedorchak, S. R. Little and J. J. McCarthy, *Langmuir*, 2015, **31**, 898–905.
- 31 N. Bowden, M. Weck, I. S. Choi and G. M. Whitesides, *Acc. Chem. Res.*, 2001, **34**, 231–8.
- 32 Y. a Diaz Fernandez, T. a Gschneidtnr, C. Wadell, L. H. Fornander, S. Lara Avila, C. Langhammer, F. Westerlund and K. Moth-Poulsen, *Nanoscale*, 2014, **6**, 14605–16.
- 33 M. Boncheva and G. M. Whitesides, *MRS Bull.*, 2005, **30**, 736–742.
- 34 N. D. Petkovich and A. Stein, *Chem. Soc. Rev.*, 2013, **42**, 3721–39.
- 35 A. Stein, B. E. Wilson and S. G. Rudisill, *Chem. Soc. Rev.*, 2013, **42**, 2763–803.
- 36 M. Maldovan, *Nature*, 2013, **503**, 209–17.
- 37 O. Carvente, G. G. Peraza-Mues, J. M. Salazar and J. C. Ruiz-Suárez, *Granul. Matter*, 2012, **14**, 303–308.
- 38 G. M. Whitesides and M. Boncheva, *Proc. Natl. Acad. Sci. U. S. A.*, 2002, **99**, 4769–74.
- 39 R. Kubo, *Reports Prog. Phys.*, 2002, **29**, 255–284.
- 40 X. C. Jiang, Q. H. Zeng, C. Y. Chen and a. B. Yu, *J. Mater. Chem.*, 2011, **21**, 16797.
- 41 Y. Li, T. Kunitake and S. Fujikawa, *Colloids Surfaces A Physicochem. Eng. Asp.*, 2006, **275**, 209–217.
- 42 A. Yethiraj, *Soft Matter*, 2007, **3**, 1099.
- 43 S.-W. Choi, I. W. Cheong, J.-H. Kim and Y. Xia, *Small*, 2009, **5**, 454–9.
- 44 K. J. Lee, J. Yoon, S. Rahmani, S. Hwang, S. Bhaskar, S. Mitragotri and J. Lahann, *Proc. Natl. Acad. Sci. U. S. A.*, 2012, **109**, 16057–62.
- 45 Y. S. Zhang, J. Yao, L. V Wang and Y. Xia, *Polymer (Guildf.)*, 2014, **55**, 445–452.
- 46 S. K. Y. Tang, R. Derda, A. D. Mazzeo and G. M. Whitesides, *Adv. Mater.*, 2011, **23**, 2413–2418.
- 47 N. A. Kotov, Y. Liu, S. Wang and C. Cumming, *Langmuir*, 2004, **20**, 7887–7892.
- 48 Y. Liu, S. Wang, J. W. Lee and N. A. Kotov, *Chem. Mater.*, 2005, **17**, 4918–4924.
- 49 H. M. Santos, C. Lodeiro and J.-L. Capelo-Martinez, in *Ultrasound in Chemistry: Analytical Applications*, ed. José-Luis Capelo-Martínez, 1998, vol. 17, pp. 17–20.
- 50 Y. Zhang, S. Wang, M. Eghtedari, M. Motamedi and N. A. Kotov, *Adv. Funct. Mater.*, 2005, **15**, 725–731.
- 51 M. J. Cuddihy and N. A. Kotov, *Tissue Eng. Part A*, 2008, **14**, 1639–49.
- 52 J. E. Nichols, J. Cortiella, J. Lee, J. A. Niles, M. J. Cuddihy, S. Wang, J. Bielitzki, A. Cantu, R. Mlcak, E. Valdivia, R. Yancy, M. L. McClure and N. A. Kotov, *Biomaterials*, 2009, **30**, 1071–9.
- 53 M. J. Cuddihy, Y. Wang, C. Machi, J. H. Bahng and N. A. Kotov, *Small*, 2013, **9**, 1008–15.
- 54 J. Lee, G. D. Lilly, R. C. Doty, P. Podsiadlo and N. A. Kotov, *Small*, 2009, **5**, 1213–21.
- 55 M. H. Lash, J. C. Jordan, L. C. Blevins, M. V. Fedorchak, S. R. Little and J. J. McCarthy, *Angew. Chem. Int. Ed. Engl.*, 2015.
- 56 S.-W. Choi, J. Xie and Y. Xia, *Adv. Mater.*, 2009, **21**, 2997–3001.
- 57 S.-W. Choi, Y. Zhang, S. Thomopoulos and Y. Xia, *Langmuir*, 2010, **26**, 12126–31.
- 58 A. N. Stachowiak, A. Bershteyn, E. Tzatzalos and D. J. Irvine, *Adv. Mater.*, 2005, **17**, 399–403.
- 59 A. N. Stachowiak and D. J. Irvine, *J. Biomed. Mater. Res. A*, 2008, **85**, 815–28.

## REVIEW

## Soft Matter

- 60 Y. Zhang, S.-W. Choi and Y. Xia, *Macromol. Rapid Commun.*, 2012, **33**, 296–301.
- 61 Y. Nahmad-Molinari and J. Ruiz-Suárez, *Phys. Rev. Lett.*, 2002, **89**, 264302.
- 62 Z. Cheng, W. Russel and P. Chaikin, *Nature*, 1999, **401**, 893–896.
- 63 O. Carvente and J. Ruiz-Suárez, *Phys. Rev. Lett.*, 2005, **95**, 018001.
- 64 A. Panaitescu and A. Kudrolli, *Phys. Rev. E*, 2014, **90**, 1–7.
- 65 J. Chopin and A. Kudrolli, *Phys. Rev. Lett.*, 2011, **107**, 1–5.
- 66 J. Olafsen and J. Urbach, *Phys. Rev. Lett.*, 1998, **81**, 4369–4372.
- 67 A. Yu, X. An, R. P. Zou, R. Y. Yang and K. Kendall, *Phys. Rev. Lett.*, 2006, **97**, 265501.
- 68 C. X. Li, X. Z. An, R. Y. Yang, R. P. Zou and A. B. Yu, *Powder Technol.*, 2011, **208**, 617–622.
- 69 O. Pouliquen, M. Nicolas and P. D. Weidman, *Phys. Rev. Lett.*, 1997, **79**, 3640–3643.
- 70 A. Panaitescu, K. A. Reddy and A. Kudrolli, *Phys. Rev. Lett.*, 2012, **108**, 1–5.
- 71 T. C. Hales, *J. Comput. Appl. Math.*, 1992, **44**, 41–76.
- 72 E. R. Chen, D. Klotsa, M. Engel, P. F. Damasceno and S. C. Glotzer, *Phys. Rev. X*, 2014, **4**, 011024.
- 73 A. Donev, I. Cisse, D. Sachs, E. a. Variano, F. H. Stillinger, R. Connelly, S. Torquato and P. M. Chaikin, *Science*, 2004, **303**, 990–993.
- 74 S. Torquato, T. M. Truskett and P. G. Debenedetti, 2000, **2**, 6.
- 75 S. M. Allen and E. L. Thomas, *The Structure of Materials*, 1999.
- 76 V. Prasad, D. Semwogerere and E. R. Weeks, *J. Phys. Condens. Matter*, 2007, **19**, 113102.
- 77 N. W. Mueggenburg, H. M. Jaeger and S. R. Nagel, *Phys. Rev. E - Stat. Nonlinear, Soft Matter Phys.*, 2002, **66**, 1–9.
- 78 N. Sushko and P. Van Der Schoot, *Phys. Rev. E - Stat. Nonlinear, Soft Matter Phys.*, 2005, **72**, 6–9.
- 79 E. Nowak, J. Knight, E. Ben-Naim, H. Jaeger and S. Nagel, *Phys. Rev. E*, 1998, **57**, 1971–1982.
- 80 Y. K. Koh, L. K. Teh and C. C. Wong, *Most*, 2004.
- 81 Y. K. Koh and C. C. Wong, 2005.
- 82 Q. Chen, L. Zhu, C. Zhao, Q. Wang and J. Zheng, *Adv. Mater.*, 2013, **25**, 4171–6.
- 83 K. Singh and M. Tirumkudulu, *Phys. Rev. Lett.*, 2007, **98**, 1–4.
- 84 O. Cedex and L. Limat, *Phys. Rev. Lett.*, 1995, **74**, 2981–2985.
- 85 W. Han, B. Li and Z. Lin, *ACS Nano*, 2013, **7**, 6079–6085.
- 86 C. H. Yi, Y. Liu, T. De Miao, Q. S. Mu and Y. L. Qi, *Granul. Matter*, 2007, **9**, 195–203.
- 87 N. D. Petkovich and A. Stein, *Chem. Soc. Rev.*, 2013, **42**, 3721–39.
- 88 H. Iddir, H. Arastoopour and C. M. Hrenya, *Powder Technol.*, 2005, **151**, 117–125.
- 89 U. G. K. Wegst, H. Bai, E. Saiz, A. P. Tomsia and R. O. Ritchie, *Nat. Mater.*, 2014, **14**, 23–36.
- 90 Z. Zhang, Y.-W. Zhang and H. Gao, *Proc. Biol. Sci.*, 2011, **278**, 519–25.
- 91 N. Brun, S. R. S. Prabakaran, C. Surcin, M. Morcrette, H. Deleuze, M. Birot, O. Babot, M. F. Achard and R. Backov, *J. Phys. Chem. C*, 2012, **116**, 1408–1421.
- 92 G. Singh, S. Pillai, A. Arpanaei and P. Kingshott, *Adv. Funct. Mater.*, 2011, **21**, 2556–2563.
- 93 J. Wang, Q. Li, W. Knoll and U. Jonas, *J. Am. Chem. Soc.*, 2006, **128**, 15606–7.
- 94 Z. Cai, J. Teng, Y. Wan and X. S. Zhao, *J. Colloid Interface Sci.*, 2012, **380**, 42–50.
- 95 E. C. M. Vermolen, A. Kuijk, L. C. Fillion, M. Hermes, J. H. J. Thijssen, M. Dijkstra and A. van Blaaderen, *Proc. Natl. Acad. Sci. U. S. A.*, 2009, **106**, 16063–16067.
- 96 L. Fillion, M. Hermes, R. Ni, E. C. M. Vermolen, a. Kuijk, C. G. Christova, J. C. P. Stiefelhagen, T. Vissers, a. Van Blaaderen and M. Dijkstra, *Phys. Rev. Lett.*, 2011, **107**, 1–4.
- 97 N. Vogel, L. de Viguerie, U. Jonas, C. K. Weiss and K. Landfester, *Adv. Funct. Mater.*, 2011, **21**, 3064–3073.
- 98 X. Huang, J. Zhou, M. Fu, B. Li, Y. Wang, Q. Zhao, Z. Yang, Q. Xie and L. Li, *Langmuir*, 2007, **23**, 8695–8.

## Soft Matter

## REVIEW

- 99 R. Radhakrishnan and B. L. Trout, *Handb. Mater. Model.*, 2005, **1**, 1613–1626.
- 100 P. Kumnorkaew, Y.-K. Y. Ee, N. Tansu and J. F. Gilchrist, *Langmuir*, 2008, **24**, 12150–7.
- 101 U. Gasser, E. R. Weeks, A. Schofield, P. N. Pusey and D. A. Weitz, *Science*, 2001, **292**, 258–62.
- 102 A. R. Kansal, T. M. Truskett and S. Torquato, *J. Chem. Phys.*, 2000, **113**, 4844–4851.
- 103 M. D. Rintoul and S. Torquato, *J. Chem. Phys.*, 1996, **105**, 9258.
- 104 B. Klumov, Y. Jin and H. Makse, *Soft Condens. Matter*, 2013, 1–7.
- 105 C. R. Wassgren, M. L. Hunt, P. J. Freese, J. Palamara and C. E. Brennen, *Phys. Fluids*, 2002, **14**, 3439–3448.
- 106 N. Boechler, G. Theocharis and C. Daraio, *Nat. Mater.*, 2011, **10**, 665–668.
- 107 C. Daraio, V. F. Nesterenko, E. B. Herbold and S. Jin, *Phys. Rev. E - Stat. Nonlinear, Soft Matter Phys.*, 2006, **73**, 1–10.
- 108 C. Li and L. Qi, *Adv. Mater.*, 2010, **22**, 1494–7.
- 109 A. Vantomme, A. Léonard, Z. Y. Yuan and B. L. Su, *Colloids Surfaces A Physicochem. Eng. Asp.*, 2007, **300**, 70–78.
- 110 E. DeGiuli, G. Düring, E. Lerner and M. Wyart, 2014, 14.
- 111 A. Haji-Akbari, M. Engel, A. S. Keys, X. Zheng, R. G. Petschek, P. Palffy-Muhoray and S. C. Glotzer, *Nature*, 2009, **462**, 773–777.
- 112 P. Richard, M. Nicodemi and R. Delannay, *Nat. Mater.*, 2005, 121–128.
- 113 D. B. Cines, T. Lebedeva, C. Nagaswami, V. Hayes, W. Massefski, R. I. Litvinov, L. Rauova, T. J. Lowery and J. W. Weisel, *Blood*, 2014, **123**, 1596–1603.
- 114 Y. S. Zhang, S.-W. Choi and Y. Xia, *Soft Matter*, 2013, **9**, 9747.
- 115 C. F. C. João, J. M. Vasconcelos, J. C. Silva and J. P. Borges, *Tissue Eng. Part B. Rev.*, 2014, **20**, 437–54.
- 116 J. Lee, M. J. Cuddihy, G. M. Cater and N. A. Kotov, *Biomaterials*, 2009, **30**, 4687–94.
- 117 T. K. Nguyen, O. Carpentier, P. Herin and P. Hivart, *Transp. Porous Media*, 2012, **96**, 255–270.
- 118 S. Shanbhag, J. Woo Lee and N. A. Kotov, *Biomaterials*, 2005, **26**, 5581–5.
- 119 Y. Zhang, K. Regan and Y. Xia, *Macromol. Rapid Commun.*, 2013, **34**, 485–91.
- 120 K. Takagi, T. Takahashi, K. Kikuchi and A. Kawasaki, *J. Eur. Ceram. Soc.*, 2010, **30**, 2049–2055.
- 121 X. Cai, Y. Zhang, L. Li, S.-W. Choi, M. R. MacEwan, J. Yao, C. Kim, Y. Xia and L. V Wang, *Tissue Eng. Part C. Methods*, 2013, **19**, 196–204.
- 122 F. M. Klenke, Y. Liu, H. Yuan, E. B. Hunziker, K. a Siebenrock and W. Hofstetter, *J. Biomed. Mater. Res. A*, 2008, **85**, 777–86.
- 123 S.-W. Choi, Y. Zhang and Y. Xia, *Langmuir*, 2010, **26**, 19001–6.
- 124 S. Zhu, D. Zhang, Z. Chen, G. Zhou, H. Jiang and J. Li, *J. Nanoparticle Res.*, 2010, **12**, 2445–2456.
- 125 Y. M. Soliman, M. F. Su, Z. C. Leseman, C. M. Reinke, I. El-Kady and R. H. Olsson, *Appl. Phys. Lett.*, 2010, **97**, 45–47.
- 126 K. Strandburg, F. Prinz and R. H. Swendsen, *Phys. Rev. Lett.*, 1987, **58**, 1038–1040.
- 127 M. J. Metzger, B. Remy and B. J. Glasser, *Powder Technol.*, 2011, **205**, 42–51.
- 128 S. K. Chung and S. K. Cho, *Microfluid. Nanofluidics*, 2008, **6**, 261–265.

## Biographies



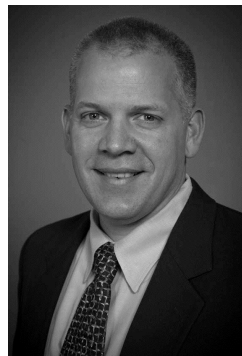
Melissa Lash graduated as a James J. Slade Scholar from Rutgers University in 2011 with a B.S. in Chemical and Biochemical Engineering. She is currently a Chemical Engineering PhD candidate at the University of Pittsburgh in the laboratories of Dr. Steven Little and Dr. Joseph McCarthy and a University of Pittsburgh Provost's Fellow. Her thesis focuses on the assembly of non-Brownian particles for the production of hierarchical materials.

## REVIEW

Soft Matter



Dr. Morgan Fedorchak received her Ph.D. in Bioengineering from the University of Pittsburgh in 2011. She is currently a Research Assistant Professor of Chemical and Petroleum Engineering at the University of Pittsburgh with additional appointments in the Department of Ophthalmology and Clinical and Translational Science. Her research focuses on the design and testing of controlled release systems and biomaterials, in particular the application of such materials to ophthalmic drug delivery and ocular diseases.



Dr. Joseph J. McCarthy received his Ph.D. in Chemical Engineering from Northwestern University in 1998. He is currently the William Kepler Whiteford Professor and Vice Chair for Education of the Department of Chemical and Petroleum Engineering at the University of Pittsburgh. The focus of Professor McCarthy's research is in transport phenomena in particulate and / or multi-phase systems and his work has impacted a number of sub-fields within Particle Technology including mixing and segregation, flow and mixing of cohesive particles, heat transfer in particle flows, and discrete modelling of particulate systems.



Dr. Steven Little received his Ph.D. in Chemical Engineering at the Massachusetts Institute of Technology in 2005. He currently holds the position of Associate Professor, CNG Faculty Fellow, and Chairman of the Department of Chemical and Petroleum Engineering at the University of Pittsburgh. He also holds appointments in the Departments of Bioengineering, Immunology, Ophthalmology and the McGowan Institute for Regenerative Medicine. His laboratory focuses on advanced drug-delivery strategies, including nano- and microparticulate controlled release systems and biomimetic systems, as applied to both immunotherapeutics and tissue regeneration.